Metastable metallic state and hysteresis below the metal-insulator transition in $PrNiO_3$

X. Granados, J. Fontcuberta, and X. Obradors
Institut de Ciència de Materials de Barcelona, Consejo Superior de Investigaciones Científicas, Campus Universitat Autònoma de Barcelona, 08193 Bellaterra, Spain

J. B. Torrance
IBM Research Division, Almaden Research Center, 650 Harry Road, San Jose, California 95120-6099
(Received 17 July 1992)

We report detailed measurements of the temperature dependence of the electrical resistivity and Seebeck coefficient for $PrNiO_3$ with particular attention to the metal-insulator (MI) transition ($T_{MI} \approx 130$ K). The Seebeck coefficient in the metallic and semiconducting phases is negative, thus indicating that the majority of charge carriers are electronlike in both phases. At low temperature ($T < 70$ K) the electrical resistivity and the Seebeck coefficient display a semiconducting behavior with an activation energy of about 22 meV. In the intermediate temperature range (70–130 K) the electrical transport data are extremely hysteretic due to the first-order character of the MI transition. Analysis of the transport properties has allowed us to extract the nucleation rate of the minority phase across the MI transition. It is shown that the metallic phase coexists with the insulating phase down to ≈ 70 K. It is suggested that the temperature at which the phase transformation takes place should be strongly dependent on pressure.

I. INTRODUCTION

Since the discovery[1] of superconductivity in the HTSC cuprates there has been a renewed interest in oxide systems, especially the late transition-metal oxides. Of particular interest has been the observation of a metallic-insulator (MI) transition in some simple perovskites of $LNiO_3$ (L = La, Pr, Nd, Sm, Eu).[2–4] Estimates of the relevant energies determining the band gap in the electronic structure, i.e., the d-d Coulomb U energy and the charge-transfer energy Δ in these oxides,[3,5] has led to the conclusion that the gap has a charge-transfer origin ($\Delta \ll U$).[2] If these estimates are correct, the transition from the insulating to the metallic phase will occur by the closing of the charge-transfer gap.[4]

It is well established that the MI transition is of first order[4,6] and the transition temperature T_{MI} rises systematically as the size of the rare earth decreases.[2,4] For L = La the system remains metallic down to 1.5 K, whereas for L = Pr, Nd, Sm, and Eu electron localization occurs at 135, 200, 400, and 460 K, respectively. Recent neutron-diffraction experiments[6] on Pr and Nd have shown that the MI transition is accompanied by small structural changes that take place at T_{MI}. The first-order character of the electronic transition is shown by the sudden, although small ($\leq 0.25\%$) volume expansion of the lattice when electron localization occurs.[6] It has also been shown that across the MI transition, expansion of the Ni-O bond length due to loss of metallic bonding leads to a slight tilt of the Ni-O-Ni angles ($\Delta\theta_{MI} \approx -0.5°$).

Neutron-diffraction data have also revealed that in $PrNiO_3$ and $NdNiO_3$ below T_{MI} some extra weak reflections of magnetic origin appear.[7] However, in the highly distorted compounds such as $SmNiO_3$ and $EuNiO_3$ there is a clear separation between the metal-insulator transition and the Néel temperature.[4] Therefore, the possibility of a band gap of af origin in this family of oxides seems to be unlikely although at the present stage it cannot be completely disregarded. On the other hand, in $PrNiO_3$ and $NdNiO_3$ the saturated magnetic moments are consistent with the Ni^{III} low-spin state for nickel rather than high-spin Ni^{+2} and holes on the oxygen sites.[2,7]

In order to understand the nature of the band gap and to build up the appropriate ground state for the electronic structure, it is important to know the character of the majority charge carriers in both the metallic and the insulating phases and the magnitude of the gap. However, in this regard, no data have yet been reported, and consequently transport measurements are needed to get a deeper insight into the electronic properties of these materials.

Associated with the first-order MI transition, a coexistence of the high-temperature metallic phase and the low-temperature semiconductor phase over a certain temperature range close to the MI transition could be expected, thus leading to a hysteretic behavior of the transport properties. Analysis of the transport coefficients in the hysteretic region can provide an estimate of the relative thermodynamic stability of both phases. The coexistence of the metallic and insulating phases may be relevant to the interpretation of several experimental results, and it is important to evaluate to which extent both phases coexist.

In this paper we report detailed measurements of the

electrical resistivity and Seebeck coefficient across the MI transition in ceramic $PrNiO_3$ pellets. We will show that charge carriers are electronlike and their character does not change across the transition. As expected, transport data clearly reveal hysteresis effects. We will use the experimental data to show that there is a wide temperature range, of about 60 K, well below the onset of the MI transition, where metallic regions of the sample coexist with semiconducting ones. Moreover, we will show that the rate of the MI phase transformation can be extracted in a consistent way from both Seebeck and conductivity data.

II. EXPERIMENT

$PrNiO_3$ powder was prepared by synthesis under high oxygen pressure. Details of the synthesis can be found elsewhere.[2] X-ray- and neutron-diffraction experiments show that the material is well crystallized, single phase, and has a perovskite structure.[2] The ideal cubic symmetry of the perovskite is slightly distorted leading to a lower symmetry structure. Extensive structure analysis has been reported elsewhere.[2,6,7]

Resistance measurements were performed by the four-probe technique, inverting current polarity in order to correct the offset of the amplifiers and thermoelectric contributions. Measuring currents over the 500 nA–5 mA range were used with identical results. Measurements were done in a He closed-cycle cryostat from room temperature down to 10 K. The temperature stability during the resistance measurements is better than ± 0.05 K. All the data reported here have been taken in a measuring protocol which involves temperature sweeps with a constant cooling or heating rate of 0.3 K/min.

Seebeck measurements were performed using an experimental system developed in our laboratory in the liquid nitrogen to room-temperature range. The difference in temperature along the sample during each Seebeck measurement rises up to 2 K.

III. RESULTS

A. Electrical resistance

The general behavior of the electrical resistance versus temperature, $R(T)$, is shown in Fig. 1. These data have been recorded in a heating-up process. This picture clearly shows that above $T_{MI} \approx 130$ K, $R(T)$ has a positive slope, thus indicating a metallic behavior. At low temperature a semiconductinglike temperature dependence is observed with a sudden enhancement of the resistivity of about two orders of magnitude, in a temperature interval of less than 10 K. The onset of semiconducting behavior is extremely abrupt (see inset of Fig. 1) and the temperature $T_{MI} \approx 130$ K where the transition from metal to insulator takes place is well defined. If the data are plotted in a $\log_{10}(R)$ versus $1/T$ scale, as it is done in Fig. 2, the low-temperature part ($T < 100$ K) of the heating-up curve displays an activated behavior, which allows us to extract an activation energy of about 22 meV. Figure 2 also shows the measured resistance in the cooling-down process (recorded at the same temperature variation rate of 0.3 K/min). The hysteretic behavior of $R(T)$ is clearly observed. As it can be appreciated in Fig. 2, the temperature at which the metallic behavior is established or disappears is well defined and does not depend, within the experimental resolution, on the sense of the thermal cycle. We have not found any measurable dependence of T_{MI} on the rate of cooling or heating of the sample. At temperatures below ≈ 70 K no trace of hysteresis is observed.

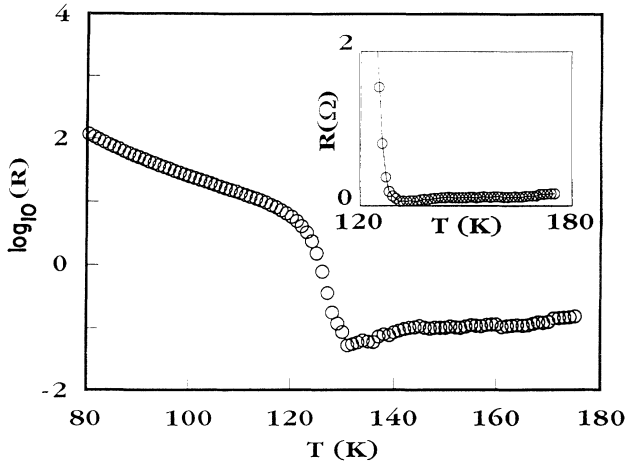

FIG. 1. Electrical resistance as a function of temperature in a warming-up process. Inset: detail of the MI transition. Logarithm is base 10.

In the temperature range between 70 and 130 K (T_{MI}) the actual value of the measured resistance depends on the lowest temperature (T_D) reached by the sample in a thermal cycle and on the time that the sample has been kept at this temperature. However, cooling the sample at

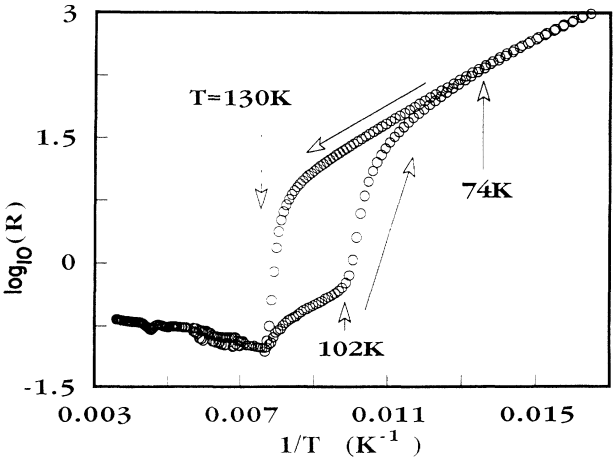

FIG. 2. Hysteresis loop of resistance. We can observe the metallic region (down 130 K); Region I (see the text) (130–102 K), which corresponds to a metallic matrix with inclusions of a nonmetallic phase; Region II (see the text) (102–74 K), which corresponds to the transition to the nonmetallic matrix with inclusions of metallic phase; and the lowest-temperature region of semiconductorlike resistance. Logarithm is base 10.

$T_D < 70$ K always leads to the same value of the resistivity at higher temperature as samples cooled at $T_D = 70$ K. See Fig. 3.

As we can see in Figs. 2 and 3, the cooling-down curve shows well-defined different sections. The metallic region extending down to 130 K is followed by a nonmetallic region (region I) of a small negative $R(T)$ slope. At $T \approx 102$ K a sudden enhancement of the absolute value of the $R(T)$ slope is observed and signals the onset of region II, where the overall resistance increases. At still lower temperatures, a semiconductorlike behavior is reached. When heating up from low temperature (see the inset of Fig. 3), the resistivity maintains a high value and the semiconductorlike behavior until the transition temperature (≈ 130 K) is reached.

When the sample is cooled down to a certain temperature and maintained at this temperature, the electrical resistance shows a strong relaxation with a long time constant. During this relaxation, the resistivity monotonically increases. Its asymptotic value depends on temperature but is always limited by the resistance values obtained in a warming-up process from $T_D < 70$ K, as shown in Fig. 2. Consequently, the relaxation process vanishes or it is no longer observable when the temperature is higher than 130 K and lower than 70 K. It is in this interval where the hysteresis phenomenon occurs.

The initial steps of the relaxation process can be well described by a logarithmic time dependence as given by

$$R(T,t) = R_0(T)\left[1 + B(T)\ln\left[1 + \frac{t}{t_0}\right]\right], \quad (1)$$

where $B(T)$ is a measure of the relaxation rate and t_0 is the time elapsed since the relaxation process has started and the first measurement is taken. $R_0(T)$ is the first measured value of the resistance at a given temperature. In Fig. 4 we show $r(t)$ vs $\ln(1+t/t_0)$, where t_0 has been extracted from the fit of the data to Eq. (1). $r(t)$ is defined as $r(t) = [R(t) - R(t=0)]/[R(\uparrow) - R(\downarrow)]$, where $R(t=0) = R_0(T)$ is the initial value of the resistance at a given temperature and time ($t = 0$). $R(\uparrow)$ and $R(\downarrow)$ are the extreme values of $R(T)$ in a heating ($\uparrow$) -cooling ($\downarrow$) thermal cycle with $T_D < 70$ K. As expected, the relaxation rate increases when T_D decreases. This result is an indication that the difference of the Gibbs energy of the insulating and metallic phases increases when lowering the temperature.

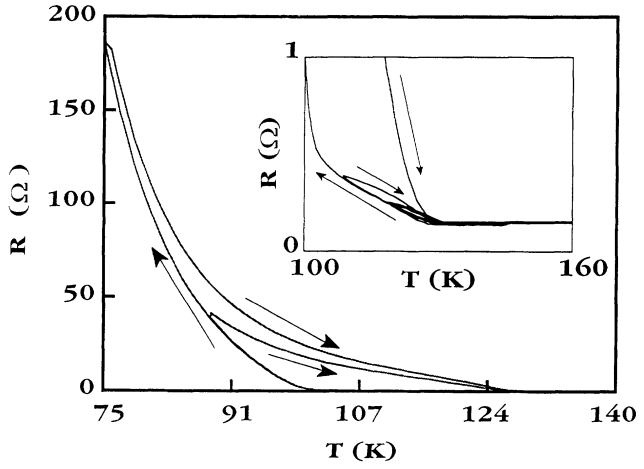

FIG. 3. Hysteresis cycles of resistance. From 160 K, the sample is cooled down to different temperatures T_D, at which the sample is maintained during 14 000 s and then heated up to 160 K. The arrows signal the sense of the thermal cycle. Examples are given for $T_D = 90$ and 70 K. Inset: Detail of the cycles for $T_D = 120$, 110, and 70 K.

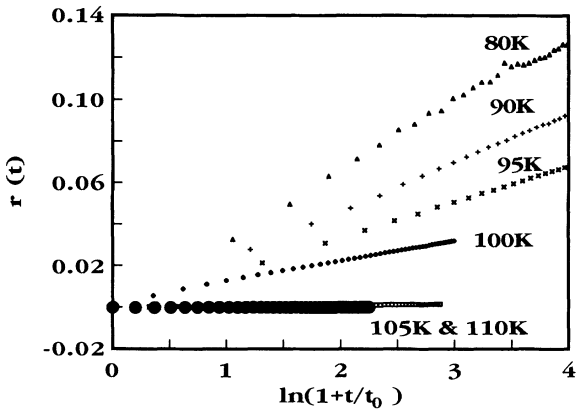

FIG. 4. Relaxation of resistance. Time dependence of the relative variation of the resistance $r(t)$. $r(t)$ is defined as the increment of resistance as a function of time divided by the difference between the values in a warming-up (from a temperature lesser than 70 K) and in a cooling-down (from 160 K) cycle, and t_0 is obtained by fitting the experimental data to Eq. (1) at each temperature.

In Fig. 5, we show the dependence of the relaxation rate $b(T)$ on temperature, where $b(T)$ is defined by

$$b(T) = \frac{d\ln[R(T,t)]}{d\ln\left[1 + \frac{t}{t_0}\right]}.$$

It can be clearly appreciated that $b(T)$ reaches max-

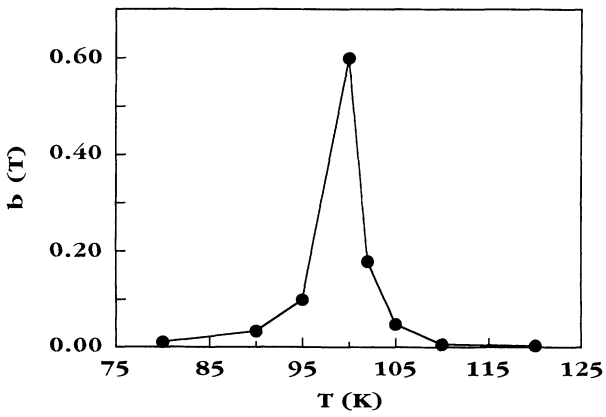

FIG. 5. Temperature dependence of the relative relaxation rate as deduced from the fit of data by Eq. (1) as a function of temperature.

imum value at $T \approx 102$ K, which is just the temperature where the resistance displays its faster temperature variation.

B. Seebeck coefficient

Figure 6 shows the Seebeck $S(T)$ coefficient measured from 160 K down to a certain temperature T_D, where the sample is kept for 14 000 s and heated again to 160 K. T_D values from 100 to 77 K were explored. For all cycles we have observed the same behavior of $S(T)$. At high temperatures, $S(T)$ has a linear dependence on temperature, it is small in magnitude and negative (≈ -10 μV/K). This behavior is typical of a metallic state with electronlike particles as charge carriers. Assuming a simple free-electron model, the observed slope of $S(T)$ in the metallic regime indicates an effective charge-carrier concentration of about 4.6×10^{20} electrons/cm^3. In the cooling-down part of the cycle, the metallic regime is observed down to $T \approx 107$ K. At lower temperature $S(T)$ decreases abruptly, becoming very large in magnitude ($S \approx -270$ μV/K at 77 K). Larger Seebeck coefficients are typical of a semiconductorlike state because of the smaller charge-carrier density. Therefore, our Seebeck data clearly reflect the MI transition. It is remarkable that in the insulating side of the transition the majority charge carriers are also electronlike. As shown by the data of Fig. 6, the Seebeck coefficient at a fixed temperature below T_{MI} changes with time, relaxing to a more negative value, in close similarity to the resistance data. In Fig. 6 (inset) the relative change ($\Delta S/S$) at a constant temperature is shown as a function of time after a cooling-down process. The enhancement of the absolute value of $S(T)$ at a constant temperature is also a manifestation of the existence of a metastable metallic state below T_{MI} and indicates that the volume of the insulating phase is steadily growing. When warming up (see Fig. 6), S decreases in magnitude again and approaches the metallic regime. However, the fully metallic state is only reached at $T \approx 130$ K, which is the temperature where the MI transition was observed in the $R(T)$ curves.

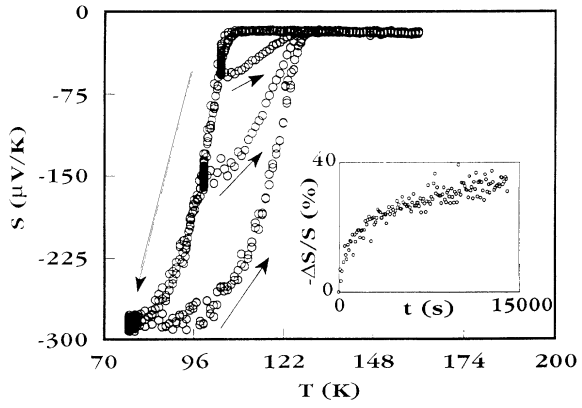

FIG. 6. Evolution of the Seebeck coefficient in cooling-heating cycles between 160 K and T_D ($T_D = 105$, 100, and 75 K). The temperature is maintained constant at T_D for 14 000 s. Inset: variation of the Seebeck coefficient upon time after a cooling-down cycle when temperature is held constant (100 K).

IV. DISCUSSION

The main results we have reported so far are the electronlike character of the majority charge carriers both in the metallic and insulating phases, and the hysteretic character of the electron-transport properties across the MI transition. The electron character of the charge carriers and the nature of the semiconducting gap are extremely interesting in their own right and will be fully discussed in a separate paper.[8] Here we will focus our attention on the hysteresis observed in the resistance and Seebeck measurements. This behavior is a manifestation of the coexistence of the insulating and metallic phases over a wide temperature interval close to the MI transition and it is a consequence of the first-order character of the transition. The fact that the temperature range where the hysteretic behavior is very broad is an indication of the similarity of the Gibbs free energy in both phases. The measured transport properties (resistance and Seebeck coefficient) are the result of the mixing of the contributions of each phase and thus they reflect the rate at which the MI transition occurs. In what follows we will analyze the data in terms of a mixture of metallic and semiconducting phases, and we will show that the overall as well as the finer details of both $R(T)$ and $S(T)$ variations can be well described by the expressions for transport properties of mixed systems.

When a system is a blend of two components with different resistivities, σ_1 and σ_2, the overall resistivity (σ^*) is basically determined by the relative volume of both phases and by the shape and distribution of the particles or domains of each phase. Several expressions have been proposed to calculate σ^* in terms of σ_i ($i=1,2$) and the relative volume V_i ($i=1,2$) of each phase.[9] The usual approximation involved in the derivation of these expressions is to assume that the "particles" are immersed in a homogeneous medium of conductivity σ'. The simplest method is to take $\sigma'=\sigma^*$, i.e., by embedding the particle in an effective medium that is constructed self-consistently. With this approximation and for the particular case of spherical particles, σ^* is given by[9]

$$V_1[(\sigma_1-\sigma^*)/(\sigma_1+2\sigma^*)] + (1-V_1)[(\sigma_2-\sigma^*)/(\sigma_2+2\sigma^*)]=0 . \quad (2)$$

In what follows we will show that this simple model can be used to describe the resistivity variations across the metallic to nonmetallic transition. Let us assume that when lowering temperature, σ_1 is the conductivity of the most conductive (metallic) phase and σ_2 is the conductivity of the more resistive (semiconductorlike) phase. According to the definitions given above, at $T_{MI}=130$ K, $V_2=0$ because of the semiconducting phase just starting to nucleate. As the temperature is further reduced, V_2 increases and thus $(\sigma^*)^{-1}$ also increases. This regime corresponds to region I in Figs. 2 and 3, and extends down to $T \approx 102$ K. At this temperature the hypothesis of a continuous metallic matrix does not hold anymore,

the percolation of the metallic matrix is broken, and the matrix become basically semiconducting. Consequently the resistivity should increase fast below this temperature. This corresponds to region II in Figs. 2 and 3 and extends down to $T \approx 70$ K, where $V_2 \approx 1$ and the matrix is a homogeneous semiconducting one.

A deeper quantitative insight into the rate at which the phase transition occurs can be obtained from Eq. (2) if one determines V_1 (or V_2) from the measured resistance. For that purpose, expressions for $\sigma_1 = \alpha R_1^{-1}$ and $\sigma_2 = \alpha R_2^{-1}$ are needed; R_1 and R_2 are the measured resistance in the metallic and semiconducting phases and α is a geometrical factor. Fitting the experimental data in the high-temperature range ($T > 130$ K) and low-temperature range ($T < 70$ K) leads to

$$R_1 = (-0.116 + 0.0016T)\ \Omega\ , \qquad R_2 = 10^{-1.19+260/T}\ \Omega\ . \tag{3}$$

Insertion of σ_1 and σ_2 into Eq. (2) determines $V_1(T)$, provided that the behavior of $R_1(T)$ and $R_2(T)$ can be extrapolated into the transition region. In Fig. 6 we show the relative volume of the metallic phase (V_1) as a function on temperature when cooling and heating respectively. According to the data of Fig. 7 it is obvious that the phase transition occurs at $T \approx 130$ K and it is at this temperature where dV/dT is maximum in both cycles. In the cooling-down curve a change of slope of $V_1(T)$ is observed at $T \approx 102$ K. We believe that this change of slope just reflects the break of the last percolating metallic path. It is worth noting in Fig. 7 that the change of slope occurs at $V_1 \approx 0.3$–0.4. This value is close to the percolation limit for a three-dimensional (3D) resistor network (≈ 0.33).[9] The rate of phase transformation decreases as T is lowered below 102 K. It is not obvious what the origin is of this slowing down of the phase transformation rate, which, however, has some similarities with typical martensitic phase transformations.[10] If this behavior does not stem from the oversimplifications involved in Eq. (2), it may be indicative that the geometrical constraints imposed by the low-temperature growing phase on the metallic phase reduce the rate of phase transformation. Following this suggestion one would expect some effect of pressure on the metastability of the metallic phase and also on T_{MI}. Indeed, some recent experiments[11] appear to support this prediction.

Data of Fig. 7 clearly reveal the hysteretic nature of the phase transformation and show that the relative concentration of insulating and metallic phases depends on the thermal cycle. As indicated, the heating-up volume fractions have been extracted from the resistivity curve obtained after cooling the sample well below 70 K. Obviously, different $V_1(T)$ would have been obtained from $R(T)$ curves recorded after cooling the sample to higher temperature.

We turn now to the Seebeck coefficient data. Our experimental results clearly show that when cooling, the metallic behavior is observed down to ≈ 105 K, where a sudden change to a semiconducting behavior takes place. Notice that the change of behavior of $S(T)$ is observed where region II is entered, i.e., when the resistivity sharply increases toward its full semiconducting value because of any remaining metallic percolating path. Explicitly, the Seebeck coefficient of a two-phase mixture, at the same level of approximation as Eq. (2), is given by[12]

$$S(T) = n_1(T)S_1(T) + n_2(T)S_2(T)\ , \tag{4}$$

where $n_i \approx \sigma_i/\sigma$ ($i = 1,2$) is the contribution to the measured conductivity (σ) of the i phase, having a conductivity σ_i and a Seebeck coefficient S_i. Down to 105 K, n_1 (for the metallic phase) is roughly two to three orders of magnitude larger than n_2 (see Fig. 2) and thus S_1 dominates the overall $S(T)$ behavior which shows a clear metallic character.

We have calculated the Seebeck coefficient $S^c(T)$ as predicted by Eq. (4), by using the experimental values of σ_i. In Fig. 8 we show the $S^c(T)$ values obtained. In this calculation we have not attempted to fit accurately the experimental data, but instead we show that the Seebeck results can be successfully interpreted in terms of a two-

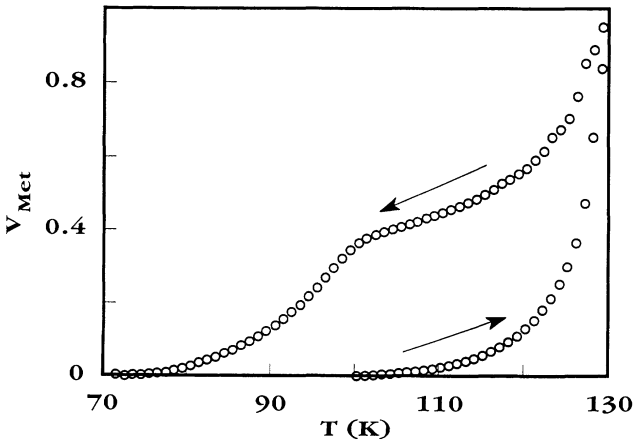

FIG. 7. Proportion of the metallic phase as a function of temperature in the cooling-down and heating-up processes as deduced from Eq. (2).

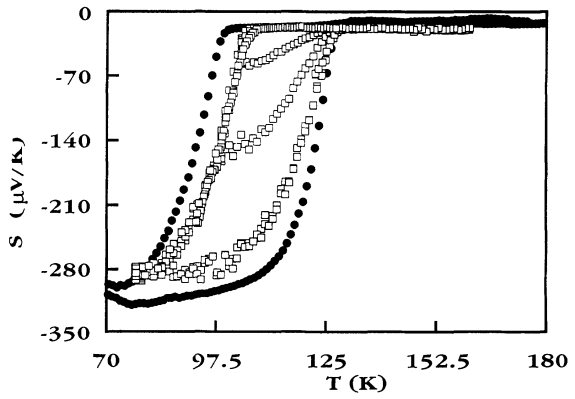

FIG. 8. The Seebeck coefficient calculated by using Eq. (4) (full symbols). The experimental data are also included for comparison (open symbols).

component mixture of materials. Consequently, we have taken $S_1(T) \approx S(130\ \text{K}) \approx -10\ \mu\text{V/K}$ and $S_2(T) \approx S_2(77\ \text{K}) \approx -300\ \mu\text{V/K}$, and we have neglected the temperature variation of S_1 and S_2 in the transition temperature region. It can be appreciated in Fig. 8 that although the model given by Eq. (4) can be somewhat crude, $S^c(T)$ closely follows the experimental data and reproduces very well the hysteresis observed in these measurements.

We can conclude that the metallic phase is present over a wide temperature range of about 60 K below the onset of the MI transition. In a heating-up process, both Seebeck and resistance measurements display abrupt changes from M to I behavior at temperatures close to $T_{\text{MI}} \approx 130$ K, but when cooling down, metallic domains coexisting with semiconducting ones severely affect the measured resistance and even dominate the Seebeck coefficient. As a result of the gradual time- and temperature-dependent rate of phase transformation, strong hysteresis effects are observed.

In summary, we have shown that Seebeck coefficient measurements indicate that in both the metallic and semiconducting phases the majority charge carriers are electronlike and their character does not change across the MI transition. In the temperature range between the onset of the phase transition ($T_{\text{MI}} \approx 130$ K) and 70 K transport properties are strongly hysteretic due to the first-order character of the transition. At $T < 70$ K a semiconductor behavior is observed with an activation energy of some 22 meV. Analysis of the transport data has allowed us to extract the relative volume of both phases which coexist over a wide temperature range (130–70 K). The rate of the MI transformation is found to be depressed below 130 K and consequently the concentration of metallic nuclei is nonzero and extends down in temperature. These experimental results suggest that pressure may severely affect the overall MI transition. In order to test such hysteresis, experiments involving transport measurements under pressure are currently being performed which we believe may shed some light on the origin of the band gap in these perovskites.

ACKNOWLEDGMENTS

Financial support from the CEE (SCI-0036-F) and the Spanish DGICYT (PB89-71) and MIDAS programs is acknowledged.

[1] J. Bednorz and K. A. Muller, Z. Phys. B **64**, 189 (1986).
[2] P. Lacorre, J. B. Torrance, J. Pannetier, A. I. Nazzal, P. W. Wang, and T. C. Huang, J. Solid State Chem. **91**, 225 (1991).
[3] J. Zaanen, G. A. Sawatzky, and J. W. Allen, Phys. Rev. Lett. **55**, 418 (1985); J. Zaanen and G. A. Sawatzky, J. Solid State Chem. **88**, 8 (1990).
[4] J. B. Torrance, P. Lacorre, A. I. Nazzal, E. J. Ansaldo, and C. H. Niedermayer, Phys. Rev. B **45**, 8209 (1992).
[5] J. B. Torrance, P. Lacorre, C. Asavaroengchai, and R. M. S. Metzger, J. Solid State Chem. **90**, 225 (1991); Physica C **182**, 351 (1991).
[6] J. L. García-Muñoz, J. Rodríguez-Carvajal, P. Lacorre, and J. P. Torrance, Phys. Rev. B **46**, 4414 (1992).
[7] J. L. García-Muñoz, J. Rodríguez-Carvajal, and P. Lacorre, Europhys. Lett. (to be published).
[8] X. Granados, J. Fontcuberta, X. Obradors, and J. B. Torrance (unpublished).
[9] P. L. Rossiter, *The Electrical Resistivity of Metals and Alloys*, edited by R. W. Cahn, E. A. Davis, and I. M. Ward, Cambridge Solid State Science Series (Cambridge University Press, Cambridge, 1991).
[10] See, for instance, S. Rubini, C. Dimitropoulos, R. Gotthardt, and F. Borsa, Phys. Rev. B **44**, 2019 (1991).
[11] X. Obradors, L. Paulius, M. B. Maple, X. Granados, J. Fontcuberta, and J. B. Torrance (unpublished).
[12] F. J. Blatt, P. A. Schroeder, and D. Greig, *Thermopower of Metals* (Plenum, New York, 1976).